ELSEVIER

Journal of Alloys and Compounds 224 (1995) 299–304

Journal of ALLOYS AND COMPOUNDS

Hydrogen evolution from cathodically charged two-phase ($Ti_3Al + TiAl$) titanium aluminides

Akito Takasaki [a], Yoshio Furuya [b], Kozo Ojima [a], Youji Taneda [a]

[a] *Department of Mathematics and Physics, National Defense Academy, 1-10-20 Hashirimizu, Yokosuka, Kanagawa 239, Japan*

[b] *Department of Technology, Faculty of Education, Nagasaki University, 1-14 Bunkyo-Machi, Nagasaki 852, Japan*

Received 3 November 1994

Abstract

Ti–45Al and Ti–50Al (at.%) titanium aluminides, whose microstructures consisted of Ti_3Al (α_2) and TiAl (γ), were cathodically hydrogen-charged in a 5% H_2SO_4 solution for charging times up to 14.4 ks (4 h), and the dissociation process of a hydride and the hydrogen evolution process during heating were investigated by thermal analyses (differential thermal analysis and thermal desorption spectroscopy). The hydride formed during cathodic charging dissociated at the temperature of about 700 K (427 °C), and corresponding to the hydride dissociation, hydrogen gas was evolved from the alloys at the dissociation temperature. In both alloys, accelerated hydrogen evolutions were observed at the lower temperatures than that for hydride dissociation. The evolution of hydrogen in the Ti–50Al alloy was extremely accelerated at about 523 K (250 °C) and the Ti–45Al at about 600 K (323 °C). The difference in the accelerated evolution temperatures was strongly dependent on the microstructures, in which structural imperfections, such as microvoids or internal cracks, could be formed during cathodic charging. The Ti–45Al alloy picked up about 1.5-times as much hydrogen as the Ti–50Al alloy, and more than 80% of the hydrogen was concentrated at the surface layer up to 20 μm in depth from the surface of the sample.

Keywords: High-temperature alloys; Hydrogen absorption; Titanium aluminides

1. Introduction

Titanium aluminides have attractive specific properties including strength at elevated temperatures and creep resistance [1]. Recently, considerable effort has been directed towards determining the hydrogen susceptibility of Ti_3Al (α_2) and TiAl (γ) alloys. Several hydride phases have been reported to form in titanium aluminides either by cathodic charging [2–8] or by charging in hydrogen gas atmosphere [8–16]. Most of the hydrides reported so far are focused on α_2-based alloys and fewer in two-phase ($\alpha_2 + \gamma$) alloys or single γ alloys. The γ and the δ type hydrides in the titanium-hydrogen system [3,8] and a $(Ti_3Al)H$ ternary hydride [4] have been reported to form in α_2-based alloys during cathodic charging. The hydride reported for γ-based alloys, on the other hand, are ternary type hydrides [6,7]. We have recently reported that a hydride, presumably $(TiAl)H_x$ ternary type, which has a tetragonal crystal structure with lattice parameters of $a = 0.452$ nm and $c = 0.326$ nm ($c/a = 0.721$), formed in two-phase ($\alpha_2 + \gamma$) titanium aluminides during cathodic charging [17,18].

This paper investigates the processes of hydride dissociation and hydrogen evolution from Ti–45Al and Ti–50Al (at.%) two-phase ($\alpha_2 + \gamma$) titanium aluminides by means of thermal analyses, i.e., differential thermal analysis (DTA) and thermal desorption spectroscopy (TDS), and the dependences of hydrogen evolution on microstructures and hydride dissociation are also discussed. There is no report on hydrogen evolution from titanium aluminides of this kind, so we believe that the results and discussion of this study would give new insight into hydrogen evolution from the alloy and the hydride dissociation.

2. Experimental procedure

The materials used for this study were Ti–45Al and Ti–50Al alloys, which were arc-melted in an argon gas atmosphere. The ingots were wrapped in tantalum foils and the Ti–45Al alloy was homogenized at 1673 K for 14.4 ks (4 h) and then annealed at 1373 K for 1.8 ks (0.5 h), and the Ti–50Al alloy at 1673 K for 14.4 ks (4 h) in an argon gas atmosphere. All ingots were

SSDI 0925-8388(95)01524-8

cooled in a furnace under an argon gas flow after heat treatment. The samples of dimensions $10 \times 10 \times 1$ mm^3 were cut from the ingots and ground with emery papers and then mechanically polished.

Hydrogen charging was performed cathodically at room temperature using platinum counter-electrodes in a 5% H_2SO_4 solution. The current density was maintained at a constant 5 kA m^{-2} and charging time was varied from 3.6 ks (1 h) to 14.4 ks (4 h) to control the hydrogen concentration in the samples.

The schematic diagram of the TDS system is shown in Fig. 1. The samples before and after hydrogen charging were mounted in a quartz tube, and the tube was pumped down to a vacuum level of 10^{-6} Pa using a turbo-molecular pump and a sputter-ion pump and then the sample was heated by a gold image furnace. During heating of the sample, total pressure and hydrogen partial pressure (ion current of H_2^+) in the system were monitored by an ionization gauge and an ULVAC MSQ-400 quadrupole mass analyzer, respectively. The measured H_2^+ ion current (A) was calibrated into hydrogen evolution rate (hydrogen molecules s^{-1}) quantitatively by flowing a known amount of an ultra-high purity (99.9999%) hydrogen gas, which was filled in a calibrated volume container, into the TDS system. The ion current monitoring was performed every 15 s from room temperature to 1173 K, so that the integrated intensity against monitoring time of TDS spectrum (hydrogen evolution rate times time) gives an actual number of hydrogen molecules evolved from the alloys; then the total hydrogen uptake (concentration) during cathodic charging could be estimated when dividing by a total sample weight. The DTA was also performed at atmospheric pressure under a nitrogen gas flow with an ULVAC TGD-7000 system. The heating rate for all measurements at this time was 20 K min^{-1}.

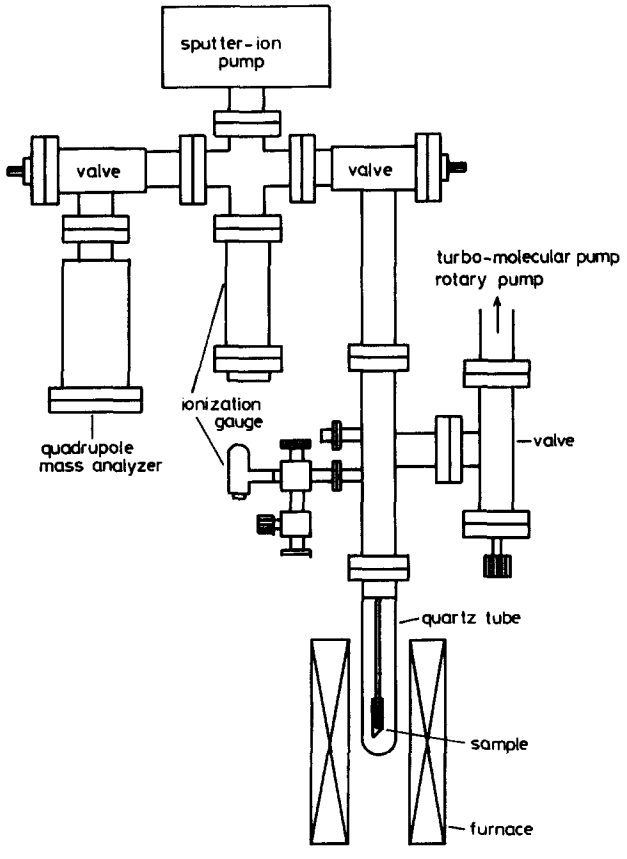

Fig. 1. Schematic diagram of thermal desorption spectroscopy system.

3. Results

The microstructures of the Ti–45Al and the Ti–50Al alloys have already been reported [18,19], but are summarized here for considering microstructural dependence on hydrogen evolution behavior. The Ti–45Al alloy showed a fully lamellar structure which consists of alternating plates of the α_2 and γ phases. The microstructure of the Ti–50Al alloy exhibited some equiaxed γ grains and grains consisting of α_2 laths sandwiched by γ bands. We have also already reported that the hydride produced during cathodic charging was stable at temperatures up to 573 K but dissociated at temperatures between 673 K and 723 K, and a longer hydrogen charging produced black hydride particles on the sample surface [17,18]. The hydride powder was carefully removed with a trimming knife from the surface of the Ti–50Al alloy charged for 14.4 ks, and thermal analyses were performed. The result of DTA for the hydride powder is shown in Fig. 2. There is a broad exothermic peak at a temperature of 700 K, which agrees well with the previous results of the high-temperature X-ray diffraction measurement [18]. Fig. 3 shows the TDS spectrum for the hydride powder [1]. The amount of the hydride powder obtained at this time is very small, so that the intensities of the TDS spectrum (hydrogen evolution rate) are relatively weak.

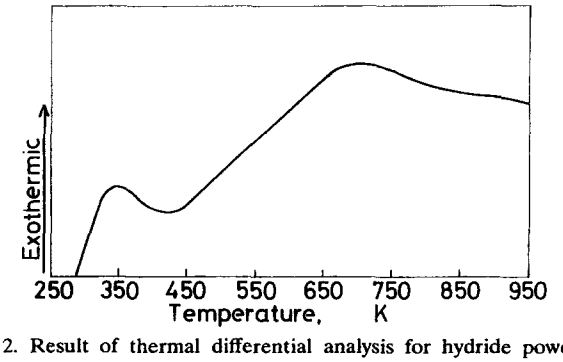

Fig. 2. Result of thermal differential analysis for hydride powder obtained from Ti–50Al alloy charged for 14.4 ks.

[1] The vertical axis (hydrogen evolution rate) in the TDS spectrum shown in Fig. 3 is not divided by sample weight, because the amount of hydride powder obtained is very small, whereas the other spectra are divided by sample weight.

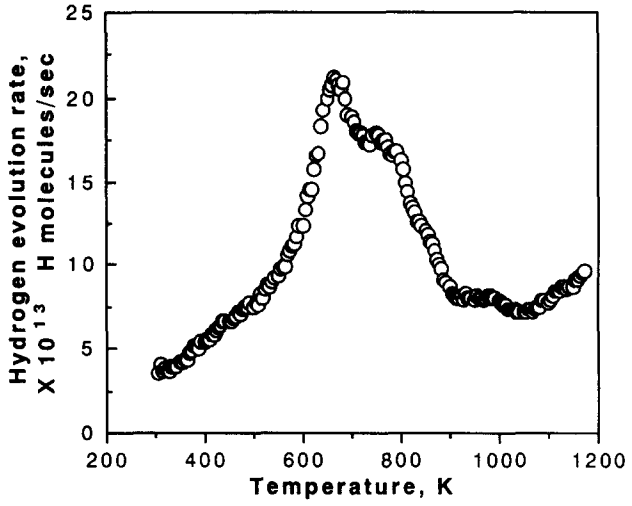

Fig. 3. Thermal desorption spectrum for hydride powder obtained from Ti–50Al alloy charged for 14.4 ks.

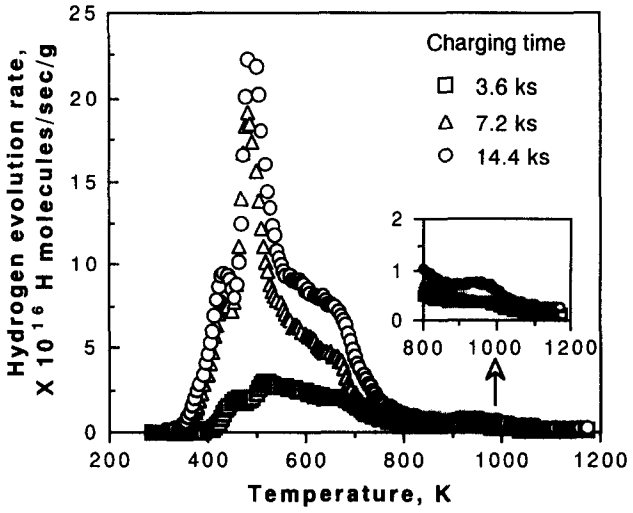

Fig. 4. Thermal desorption spectra for Ti–50Al alloys after hydrogen charging for various times.

The hydrogen evolution from the hydride begins at temperatures of less than 500 K and terminates at about 900 K. It might be found that there is more than one shoulder peak at around 900 K and an increase in hydrogen evolution at temperatures of above 1000 K. We consider that the shoulder peaks might be due to hydrogen dissolution in the alloy matrix, which is discussed later, because there is a possibility that a small amount of matrix alloy was also removed during the process of removing the hydride powder with a trimming knife, and that the increase in hydrogen evolution at temperatures of above 1000 K is due to the TDS system characteristics, which can be ignored level when there are large quantities of hydride powder. Except for these hydrogen evolutions, it is found that the strongest peak is at about 670 K, with a sub-peak at 750 K. This means that the evolution of hydrogen from the hydride is much accelerated at temperatures between 670 K and 750 K, which also agrees well with the previous results of high-temperature X-ray diffraction measurement [18] and the DTA result shown in Fig. 2. These two peaks may indicate that there are two kinds of hydrogen sites in a hydride crystal, such as octahedral or tetrahedral sites. Further work is necessary to determine the hydrogen sites.

The results of TDS analyses for the Ti–50Al alloy are shown in Fig. 4. The integrated intensities of the TDS spectra increase with charging time, which indicates that the total hydrogen concentrations (uptakes) increase with charging time. For the sample after hydrogen charging for 3.6 ks, hydrogen is evolved at about 423 K and most of the hydrogen is evolved at temperatures up to about 773 K. For the sample charged for 14.4 ks, there are, at least, four peaks (423 K, 523 K, 600 K and 700 K) in the TDS spectrum at temperatures between 400 K and 800 K, in which hydrogen evolution is very much accelerated at about 523 K (23×10^{16} molecules H s^{-1} g^{-1}). At higher temperatures than these four peaks, it is also found that there is an additional (lowest) broad peak at about 973 K. For the Ti–45Al alloy (Fig. 5), on the other hand, the total hydrogen concentrations also increase with charging time. The accerelated evolution of hydrogen at 523 K as observed for the Ti–50Al alloy is not observed in the Ti–45Al alloy, and there also seem to be four peaks, at least, in the TDS spectra at temperatures between 400 K and 800 K, particularly for the sample charged for 14.4 ks, but it is difficult to separate the peaks at this time. The additional peak at 973 K as observed in the Ti–50Al alloy cannot be observed in the Ti–45Al alloy due to the higher background level. These evolution peaks (temperatures) are considered to participate closely in the microstructures, cracks produced during cathodic charging, hydride and normal dissolution of hydrogen in matrix, and will be discussed later. In the

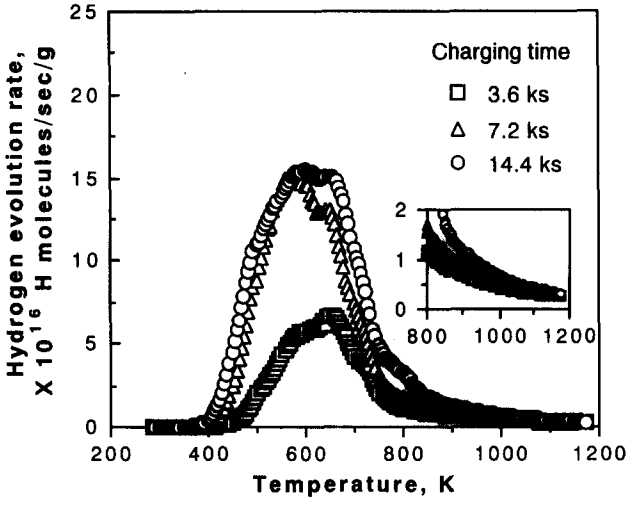

Fig. 5. Thermal desorption spectra for Ti–45Al alloys after hydrogen charging for various times.

TDS analyses, the samples were not heated to their melting temperature but were heated to 1173 K. The hydrogen evolution is under background levels at temperatures above 1073 K, so that the actual hydrogen concentrations (or uptakes) can be estimated from the integrated intensities of each TDS spectrum.

The total hydrogen concentrations in the Ti–50Al and the Ti–45Al alloys as a function of charging time are shown in Fig. 6. For both alloys, the hydrogen concentrations increase with charging time, as mentioned earlier, and a rapid increase in hydrogen concentration is found for charging times up to 7.2 ks. It is also found that the Ti–45Al alloy picks up about 1.5-times as much hydrogen as the Ti–50Al alloy: for instance, for the alloys charged for 14.4 ks, the Ti–45Al alloy picks up about 450 wppm hydrogen whereas the Ti–50Al alloy uptakes about 300 wppm.

Fig. 7 shows the TDS spectra for the Ti–50Al alloy charged for 14.4 ks before and after removal of the surface layer of the sample [2], in which the sample surface was removed to a depth of 20 μm with an emery paper. After removal of the surface layer, the TDS peak at about 523 K is still observed, but the hydrogen evolution rate drastically decreases. The weak hydrogen evolution at about 700 K is also still observed after removal, indicating that the hydride still remains. The total hydrogen concentration in the sample after removal is about 40 wppm. Comparing with the total hydrogen concentration in the Ti–50Al alloy before removal of the surface layer, more than 80% of the hydrogen is concentrated in the outermost 20 μm of the sample.

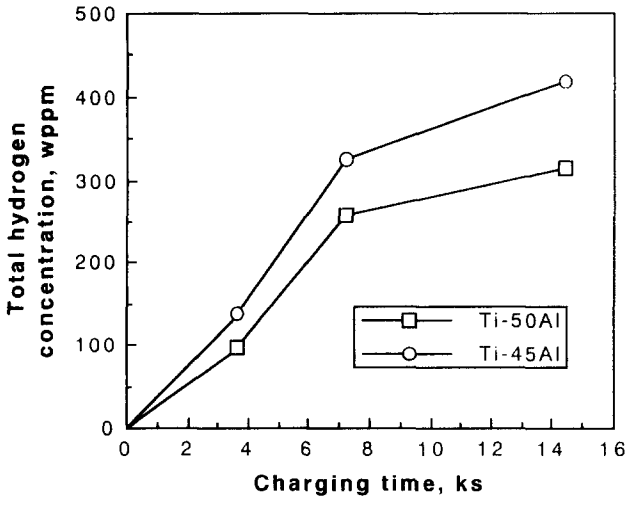

Fig. 6. Total hydrogen concentrations in Ti–45Al and Ti–50Al alloys as a function of charging times.

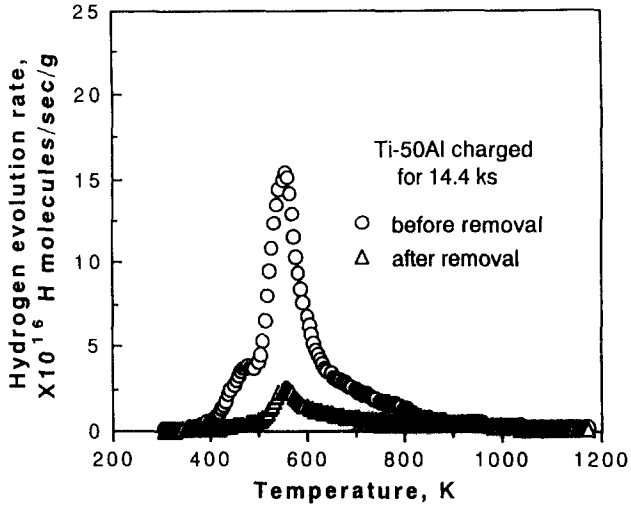

Fig. 7. Thermal desorption spectra for Ti–50Al alloy charged for 14.4 ks before and after removal of surface layer.

4. Discussion

As one of the interactions between hydrogen and metals (or alloys), it is widely understood that firstly hydrogen molecules are adsorbed physically by van der Waals force onto the surface of metals and secondly adsorbed hydrogen molecules dissociate into hydrogen atoms, then hydrogen atoms are chemically adsorbed. It is also recognized that hydrides would form when the hydrogen concentration in the metals reaches the solubility limits.

For metals and alloys whose solubility limit for hydrogen is very low or where hydrides would not form, such as iron, nickel and iron alloy [20–23], the hydrogen trapping phenomenon, which is attractive interactions between hydrogen atoms and structural imperfections in crystal, is more dominant than the dissolution phenomenon, and it is known that almost all kinds of defects in metals and alloys, such as dislocation, microvoid, grain boundary, phase interface and the interface of non-metallic inclusions, can act as hydrogen trapping sites [21]. Our previous work [18] indicated that cracks were observed on the surfaces of the Ti–45Al and the Ti–50Al alloys after cathodic charging, and the morphology of the cracks turned into pits after longer charging. We have also reported that cracks or pits were observed within the γ phase regions in the two-phase coexisting grains (such as lamellar grains) but not within the α_2 phase or single γ grains, which resulted in much more weight loss in the Ti–50Al alloy than the Ti–45Al alloy [18]. In the Ti–45Al and Ti–50Al alloys, hydrogen trapping due to the cracking should be also taken into consideration, as well as hydrogen

[2] The TDS spectra shown in Fig. 7 were obtained for a different sample from those used in Fig. 4. Some variations, which can be ignored, are found in total hydrogen picked up during cathodic charging and TDS peak temperatures. The deviations are considered to be due to heterogeneous distribution of hydrogen on the sample surface during cathodic charging, and this should be eliminated for samples charged by hydrogen gas.

uptakes due to normal dissolution and hydride formation.

Schematic TDS spectra are shown in Fig. 8, in which states of hydrogen (dissolution, hydride, etc.) are indicated. In our study for thermally charged Ti–45Al and Ti–50Al alloys at temperatures between 623 K and 1023 K [24], there was the strongest TDS peak at about 1000 K and no peak at temperatures of less than 650 K. No hydride was detected for the thermally charged alloys by X-ray diffractometry; thus we have considered that the strong peak at about 1000 K was due to hydrogen dissolution in the alloy matrix. The evolution peak at about 973 K, which was obtained in this study particularly for the Ti–50Al alloy, is, therefore, due to the hydrogen dissolution in normal lattice sites (matrix phases). In each alloy, the hydride has already formed after cathodic charging for 14.4 ks, then the solubility limit of hydrogen in the Ti–50Al alloy during cathodic charging is estimated to be about 6 wppm. It is difficult to estimate the solubility limit for the Ti–45Al alloy because the TDS peak temperature at about 973 K cannot be separated (see Fig. 5), but this is considered to be about the same or slightly higher than that in the Ti–50Al alloy. The (limit) solubility of hydrogen in thermally charged Ti–48Al–1V at 673 K is reported to be less than 100 wppm [25,26]. The hydrogen solubilities during cathodic charging are much smaller than those during thermal charging, because cathodic charging in this study was performed at room temperature. The TDS peak at about 700 K results from the hydride dissociation (see Fig. 3), and the integrated intensities of TDS spectra increase with charging time, indicating that the amount of the hydride increases with charging time. The lower TDS peaks (423 K and 523 K and 600 K) than the dissociation temperature of the hydride are considered to result from hydrogen trapped at structural imperfections, such as microvoids or internal cracks produced during cathodic charging, because, as mentioned above, there was no peak at temperatures of less that 650 K for the thermally charged alloys [24]. Furthermore, we have observed for a Ti–25Al alloy (α_2-based alloy) that there was a strong TDS peak at about 1000 K when cracks were not introduced but this peak disappeared and the peak at low temperatures appeared when cracks were introduced during thermal charging [27]. It is found that the intensities of these peaks are dependent on the microstructures. The sharp TDS peaks at 423 K and 523 K, which were observed in the Ti–50Al alloy, are not found in the Ti–45Al alloy, suggesting that these peaks result from the γ phase, whereas the peak at 600 K is more drastic in the Ti–45Al alloy than the Ti–50Al alloy, indicating that this peak results from the α_2 phase. When one performs TDS analysis for various heating rates, it is expected that the peak temperatures would shift depending on apparent (or trap) activation energies for evolution of hydrogen and one can classify types of trap sites of hydrogen. The deconvolution work of the TDS spectra is believed to give clearer views for separating the peaks, and the integrated intensity of the peak indicates a separate effect of hydrogen trapping. The TDS analyses for various heating rates are now in progress and the activation energies as well as the deconvolution results of these TDS spectra will be reported elsewhere.

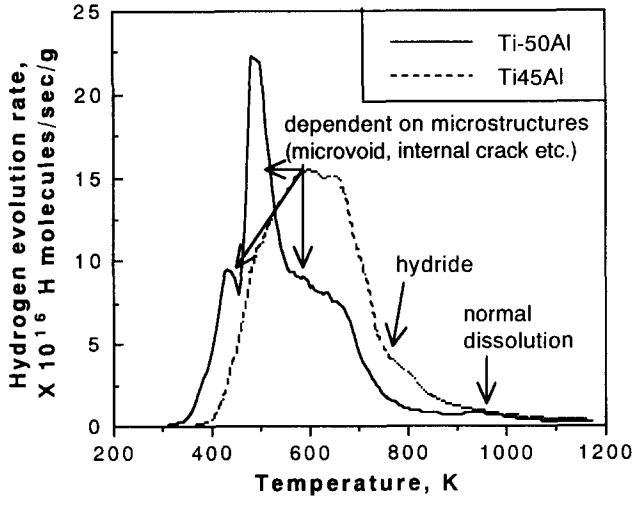

Fig. 8. Schematic thermal desorption spectra showing states of hydrogen.

In a series of the TDS analyses for the Ti–50Al and the Ti–45Al alloys, it is concluded that most of hydrogen picked up in these alloys can be easily removed by vacuum aging at temperatures above 973 K. It is also indicated that the hydride formed during cathodic charging would not limit the high-temperature applications if structural imperfections, such as cracks, were not produced, because the hydride dissociates at a temperature of about 700 K, which is significantly lower than application temperatures, but additional work should be necessary on the mechanical properties. Some hydrides reported to form in γ-based titanium aluminides during high-temperature and high-pressure hydrogen gas charging [9,16] could be different from the present hydride, because the hydride observed in this study, again, dissociates at lower temperatures than that for high-temperature hydrogen gas charging.

5. Conclusions

1. The hydride formed during cathodic charging dissociates at a temperature of about 700 K, and at the hydride dissociation temperature the evolution of hydrogen from the alloys is also accelerated.
2. The evolution of hydrogen from hydrogen-charged Ti–50Al alloy is extremely accelerated at temperatures of about 523 K, and in the Ti–45Al alloy at

temperatures of 600 K. These evolution temperatures participate in structural imperfections, such as microvoids and internal cracks, produced during cathodic charging.

3. The evolution temperature of hydrogen corresponding to the normal dissolution in the matrix is about 973 K, and the solubility limit of hydrogen during cathodic charging at room temperature is estimated to be about 6 wppm.
4. For the alloys charged for 14.4 ks, the Ti–45Al alloy picks up about 450 wppm hydrogen whereas the Ti–50Al alloy about 300 wppm, suggesting that titanium-rich alloy picks up much hydrogen.
5. The cathodic hydrogen charging concentrates more than 80% of hydrogen in the surface 20 μm of the sample.

Acknowledgment

The authors wish to thank Mr. A. Mitsuhashi, Central Research Institute of Mitsubishi Materials Corporation, for providing the homogenized ingots.

References

[1] H.A. Lipsitt, in C.C. Koch et al. (eds.), *High-Temperature Ordered Intermetallic Alloys*, Vol. 39, MRS, Pittsburgh, PA, 1985 pp. 351–364.
[2] E. Manor and D. Eliezer, *Scr. Metall. Mater., 23* (1989) 1313–1318.
[3] D. Eliezer, J. Haddad, M. Dangur and F.H. Fores, *Scr. Metall. Mater., 27* (1992) 845–859.
[4] P. Rozenak and M. Dangur, *J. Mater. Sci., 27* (1992) 2273–2278.
[5] Y. Zhang, Y. Wang, Y.B. Wang, W.Y. Chu and C.M. Hsiao, *Scr. Metall. Mater., 29* (1993) 975–980.
[6] J. Gao, Y.B. Wang, W.Y. Chu and C.M. Hsiao, *Scr. Metall. Mater., 27* (1992) 1219–1222.
[7] Y. Combres, S. Tsuyama and T. Kishi, *Scr. Metall. Mater., 27* (1992) 509–514.
[8] W.Y. Chu, A.W. Thompson and J.C. Williams, *Acta Metall. Mater., 40* (1992) 455–462.
[9] D.E. Matejczyk and C.G. Rhodes, *Scr. Metall. Mater., 24* (1990) 1369–1373.
[10] D.S. Shin, G.K. Scarr and G.E. Wasielewski, *Scr. Metall., 23* (1989) 973–978.
[11] D. Legzdina, I.M. Robertson and H.K. Birnbaum, *Scr. Metall. Mater., 26* (1992) 1737–1741.
[12] W.Y. Chu and A.W. Thompson, *Metall. Trans., 23A* (1992) 1299–1312.
[13] M. Gao, J.B. Boodey and R.P. Wei, *Scr. Metall. Mater., 24* (1990) 2135–2138.
[14] K.S. Chan, *Metall. Trans., 24A* (1993) 1095–1105.
[15] P.S. Rudman, J.J. Reilly and R.H. Wiswall, *J. Less-Common Met., 58* (1978) 231–240.
[16] D. Legzdina, I.M. Robertson and H.K. Birnbaum, *J. Mater. Res., 6* (1991) 1230–1237.
[17] A. Takasaki, K. Ojima and Y. Taneda, *Scr. Metall. Mater., 28* (1993) 1483–1487.
[18] A. Takasaki, K. Ojima and Y. Taneda, *J. Alloys Comp., 216* (1994) 1–6.
[19] A. Takasaki, K. Ojima and Y. Taneda, *Metall. Mater Trans., 25A* (1994) 2491–2496.
[20] S.M. Lee and J.Y. Lee, *Acta Metall. Mater., 35* (1987) 2695–2700.
[21] H.G. Lee and J.Y. Lee, *Acta Metall., 32* (1984) 131–136.
[22] S.M. Lee and J.Y. Lee, *Metall. Trans., 17A* (1986) 181–187.
[23] K. Hashimoto and M. Meshii, *Scr. Metall., 19* (1985) 1075–1079.
[24] A. Takasaki, Y. Furuya, K. Ojima and Y. Taneda, *Scr. Metall. Mater.*, in press.
[25] D.S. Shong, Y.W. Kim, C.F. Yolton and F.H. Froes, in C.T. Liu et al. (eds.), *High Temperature Ordered Intermetallic Alloys III*, Vol. 113, MRS, Pittsburgh, PA, 1989, pp. 711–716.
[26] J.B. Boodey, M. Gao and R.P. Wei, in R.H. Jones and R.E. Ricker (eds.), *Enviromental Effects on Advanced Materials*, TMS, Warrendale, PA, 1991, pp. 57–65.
[27] A. Takasaki, Y. Furuya, K. Ojima and Y. Taneda, unpublished work.